PAPER • OPEN ACCESS

Radiosonde studies of internal waves in the southern near-equatorial atmosphere of the Earth

To cite this article: VN Gubenko *et al* 2021 *J. Phys.: Conf. Ser.* **1991** 012012

View the article online for updates and enhancements.

Radiosonde studies of internal waves in the southern near-equatorial atmosphere of the Earth

V N Gubenko[1], I A Kirillovich[1] and V E Andreev[1]

[1] Kotel'nikov Institute of Radio Engineering and Electronics RAS (Fryazino branch), Vvedensky square 1, Fryazino 141190, Moscow region, Russia

E-mail: vngubenko@gmail.com, gubenko@fireras.su

Abstract. Radiosonde measurement data of the wind speed, conducted on 28 February and on 15 November 2007, have been used for the internal gravity waves (IGWs) identification and determination of their parameters in the Earth's lower stratosphere over Cocos Islands (coordinates: latitude $-12.04°S$ and longitude $-96.90°E$). A wind speed hodograph analysis has shown that observed fluctuations are wave-induced while the wave energy propagates upwards. Using the results of a wind speed hodograph analysis, dispersion equation and polarization relations, we have obtained the magnitudes of key IGW characteristics such as the intrinsic frequency, amplitudes of vertical and horizontal perturbations of the wind speed, vertical and horizontal wavelengths, intrinsic vertical and horizontal phase (and group) speeds, wave kinetic, potential and total energy. An original method for determining the wave ground-based frequency and azimuthal angle of IGW propagation in the Earth's atmosphere has been proposed. Application of the developed method to radiosonde measurements, conducted on 28 February 2007, has given a possibility to establish that the wave ground-based frequency is equal to $14.0 \cdot 10^{-4}$ rad/s and it corresponds to the actual wave period T=1.25 hours.

1. Introduction

An important task of atmospheric physics is the study of wave processes which determine atmospheric dynamics at all altitudes. Internal gravity waves (IGWs) are a characteristic feature of all stably stratified planetary atmospheres. Main sources of the IGWs are in the Earth's lower atmosphere where internal waves may be generated by the thermal contrasts near surface, topography, wind shear instability, convection and frontal processes. These waves can propagate upward and have a significant impact on dynamics and thermal state of the Earth's middle and upper atmosphere. Internal waves are always present in the lower and upper atmosphere, while the significance of IGWs for atmospheric dynamics is different at different altitudes. Since the wave energy is proportional to air density, then the amplitude of a conservatively propagating harmonic wave is the greater, the lower the atmospheric density. In the Earth's troposphere, the amplitudes of recorded IGWs are relatively small; however, their importance for dynamics increases with altitude, and an influence of internal waves in the middle and upper atmosphere can no longer be neglected. One of the most well known methods for studying the quasi-harmonic IGWs observed in the Earth's atmosphere by various ground-based and space means is the method of analyzing the wind speed hodograph. These means include satellite-born remote sensing techniques and rocket measurements, ground-based radar and lidar systems, radiosondes, ground-based observations of airglow and others [1–24].

Nowadays, the wind speed hodograph method is a standard working tool in meteorology. It was first applied to study inertial oscillations in the ocean [1], as well as to study IGWs in the Earth's

atmosphere [4]. An idea of the hodograph method is to track the motion of a wind speed perturbation vector with altitude. According to the IGW theory, the wind speed hodograph (trajectory described by the end of a wind speed disturbances vector) has the shape of an ellipse, the major axis of which is parallel to the direction of horizontal wave propagation. The lengths of major and minor semi-axes of this polarization ellipse are amplitudes of wind speed perturbations along the horizontal wave vector component and in the transverse direction, respectively [25, 26]. In the case when a vertical shear of background (unperturbed) wind speed is insignificant, the axial ratio (R) of the minor axis length to the major axis length for specified ellipse is equal to the ratio (f/ω) of the inertial frequency (Coriolis parameter) f to the intrinsic frequency ω of an internal wave. An elliptical approximation of the wind speed hodograph makes it possible not only to find the intrinsic wave frequency ω, but also to determine the direction of a horizontal group speed component which is parallel to the major axis of polarization ellipse [25, 26]. It should be noted that the establishment of indicated direction with an uncertainty of $\pm 180°$ is a disadvantage of the hodograph method. Therefore, for unambiguous determination of a wave frequency in the reference frame of ground-based observer, the additional simultaneous measurements of temperature or density in the Earth's atmosphere are required.

The purpose of this work is: I) development of the wind speed hodograph method for reconstructing the IGW characteristics in the reference frame of ground-based observer and determining the internal wave propagation direction in the Earth's atmosphere based on an analysis of the radiosonde wind speed measurements; II) approbation of the upgraded hodograph method for analyzing the radiosonde data in the Earth's lower stratosphere over Cocos Islands where internal waves were detected.

2. Determination of internal wave characteristics using elliptical wind speed hodograph and an analysis of radiosonde measurements in the southern near-equatorial atmosphere of the Earth

Parameters of the elliptical wave hodograph in radiosonde wind speed measurements can be found using the following relations:

$$\theta = \frac{1}{2}\arctan\frac{\left\langle 2u'_x v'_y \right\rangle}{\left\langle u'^{\,2}_x \right\rangle - \left\langle v'^{\,2}_y \right\rangle} + \frac{\pi n}{2}, \tag{1}$$

$$a^2, b^2 = \left\langle u'^{\,2}_x \right\rangle + \left\langle v'^{\,2}_y \right\rangle \pm \left[\left(\left\langle u'^{\,2}_x \right\rangle - \left\langle v'^{\,2}_y \right\rangle \right)^2 + 4\left\langle u'_x v'_y \right\rangle^2 \right]^{1/2}, \tag{2}$$

where θ is an azimuthal angle between the horizontal X-axis (W/E-direction from west to east) and the major axis of an IGW polarization ellipse (positive angle values correspond to the counterclockwise measuring of θ relative to the X-axis); n is an arbitrary integer; the values a and b represent lengths of the major and minor semi-axes of specified ellipse; the parameters u'_x and v'_y are wind speed variations in the zonal (W/E-direction) and meridional (S/N-direction from south to north) directions, respectively. Angle brackets indicate an averaging of the corresponding variable over the vertical wavelength. Expressions (1) and (2) were published earlier in the works [1, 4]. However, in both these articles, formula (1) does not contain the important term $\pi n/2$, which leads to an erroneous limitation of the interval of possible angle θ values to the range $[-\pi/4, \pi/4]$.

Registration of the radiosonde wind speed measurements in the Earth's atmosphere was carried out at intervals of 6 seconds, which corresponds to the vertical resolution of ~30 m for a mean balloon ascent speed of ~5 m/s. The accuracy of measuring the wind speed is equal to ~1 m/s [25]. Figure 1 shows profiles of the zonal (W/E-component) and meridional (S/N-component) wind speed components (panels a and b) for the interval 19.0–20.5 km obtained from radiosonde measurements on February 28, 2007 at the Earth's stratosphere over Cocos Islands. Coordinates of the sounded atmospheric region were 12.04°S (latitude) and 96.90°E (longitude). Dots indicate the background (mean) profiles calculated on the basis of polynomial approximation of initial data by the least squares method (LSM) on the selected altitude interval. Panel c in Figure 1 shows the vertical profiles of wind speed variations in the S/N- and W/E-components which were determined as the differences between

initial and mean profiles (panels a and b). Analyzing these profiles, we have determined the vertical wavelength λ_z = 800 m of the quasi-periodic wind speed disturbances at the Earth's lower stratosphere.
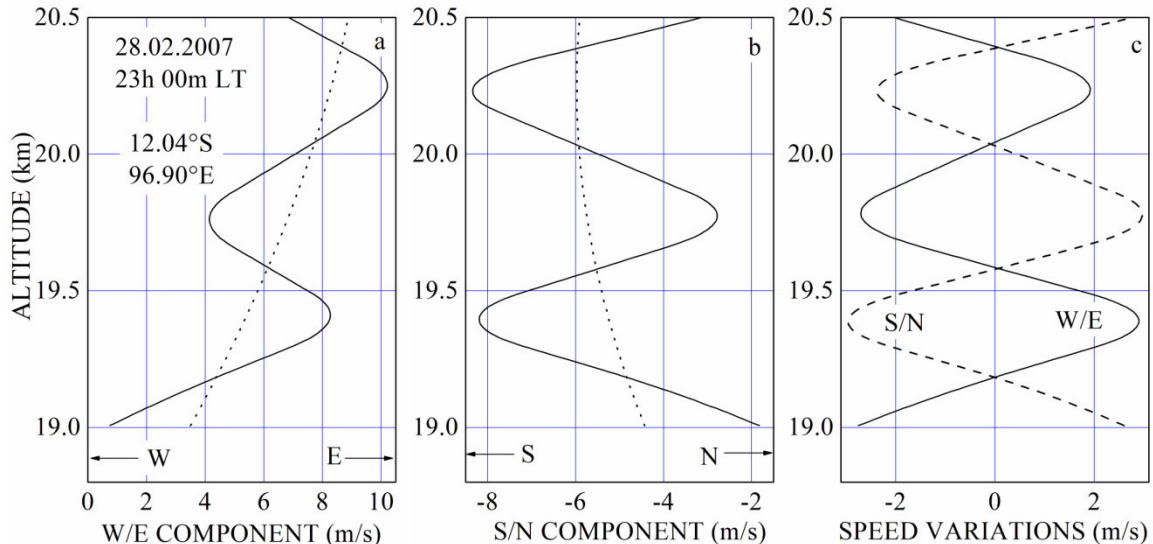

Figure 1. Altitude profiles of the zonal (W/E-component) and meridional (S/N-component) wind speed components (panels a and b) obtained from radiosonde measurements on February 28, 2007 at the Earth's stratosphere over Cocos Islands. The coordinates of sounded area and the local time (LT) of measurements are shown. Dotted lines denote the background (mean) profiles calculated using the LSM-approximation of initial data by a third-degree polynomial in the interval 19.0–20.5 km. Vertical profiles of the wind speed component variations (panel c) were determined as the differences between initial and background profiles.

In order to construct the wind speed hodograph and to determine the IGW characteristics in the radiosonde measurement session on February 28, 2007, the analyzed altitude range was divided into five altitude intervals. Each interval had a length of ~800 m (vertical wavelength) and it was vertically shifted with respect to the adjacent interval by about of ~200 m (quarter of wavelength λ_z). Figure 2 shows hodographs of horizontal wind speed variations for two altitude intervals 19.17–20.05 km (left panel) and 19.57–20.40 km (right panel). Polarization ellipses approximating the measurement data (solid lines) are shown by dashed lines in Figure 2. Lengths of the major a and minor b semi-axes of these ellipses determine the amplitudes $|u'|$ and $|v'|$ of horizontal wind speed perturbations: $|u'|$ = 3.84 m/s, $|v'|$ = 0.11 m/s (left panel) and $|u'|$ = 3.43 m/s, $|v'|$ = 0.14 m/s (right panel). For two indicated altitude intervals, the values of azimuthal θ-angle were found: θ = 133.47° (left panel) and θ = 131.27° (right panel). For the analyzed hodographs in Figure 2 it is found that the end of a wind speed variations vector rotates counterclockwise with increasing altitude. According to the internal wave theory, this corresponds to the downward phase propagation and upward wave energy transport in the Southern Hemisphere. At the next step, the Coriolis parameter value for observation point was calculated and using the axial ratio R for the considered wind speed hodograph, we have found the ratio f/ω, intrinsic frequency ω, and other IGW characteristics. To determine the wave parameters, it is necessary to have a reliable estimate of the background Brunt-Vaisala frequency N_b (stability parameter of atmospheric stratification) for the analyzed altitude interval. Applying expression (5) from the work [25] to the mean temperature profile for considered radiosonde session, we obtained the value N_b = 2.5·10^{-2} rad/s. A detailed description of the procedure for determining the wave parameters based on results of a wind speed hodograph analysis is given in the works [25, 26]. Figure 3 shows hodographs of horizontal wind speed variations in the radiosonde measurement session on February 28, 2007 for two other altitude intervals: 19.30–20.25 km (left panel) and 19.70–20.50 km (right

panel). For the fifth (bottom) altitude interval 19.00–19.80 km, we have also constructed the wind speed hodograph (it is not shown here) and determined internal wave characteristics.
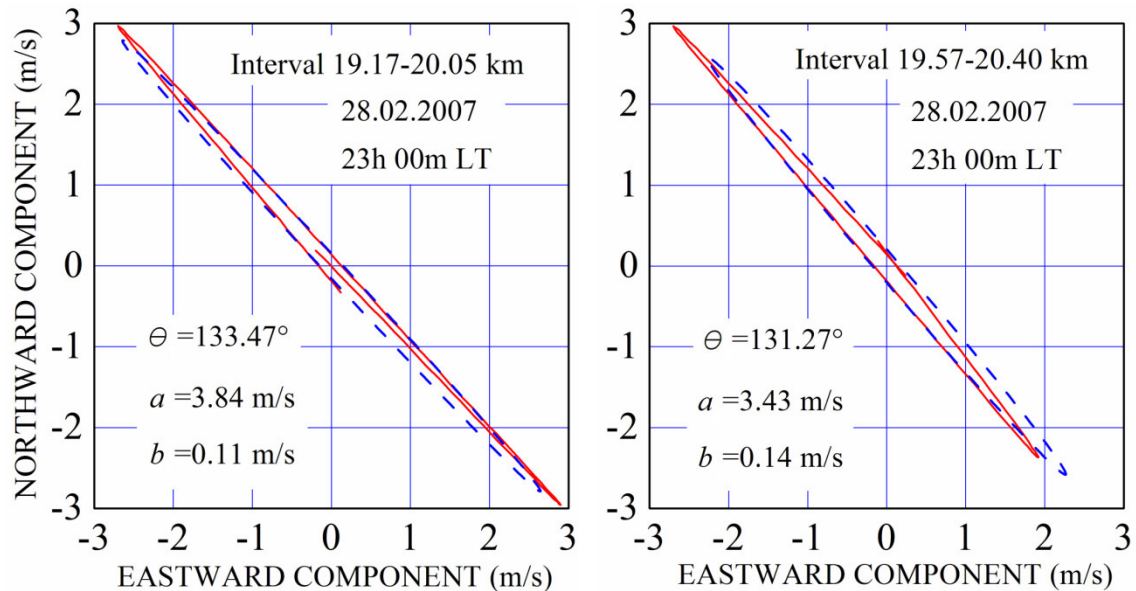

Figure 2. Results of a hodograph analysis for wind speed disturbances which were obtained from radiosonde measurements on February 28, 2007 at the Earth's stratosphere over Cocos Islands in two altitude intervals 19.17–20.05 km (left panel) and 19.57–20.40 km (right panel). Polarization ellipse approximating the measurement data (solid line) is represented by the dashed line. Lengths of major (a) and minor (b) semi-axes of ellipse and values of angle θ are also shown in this figure.
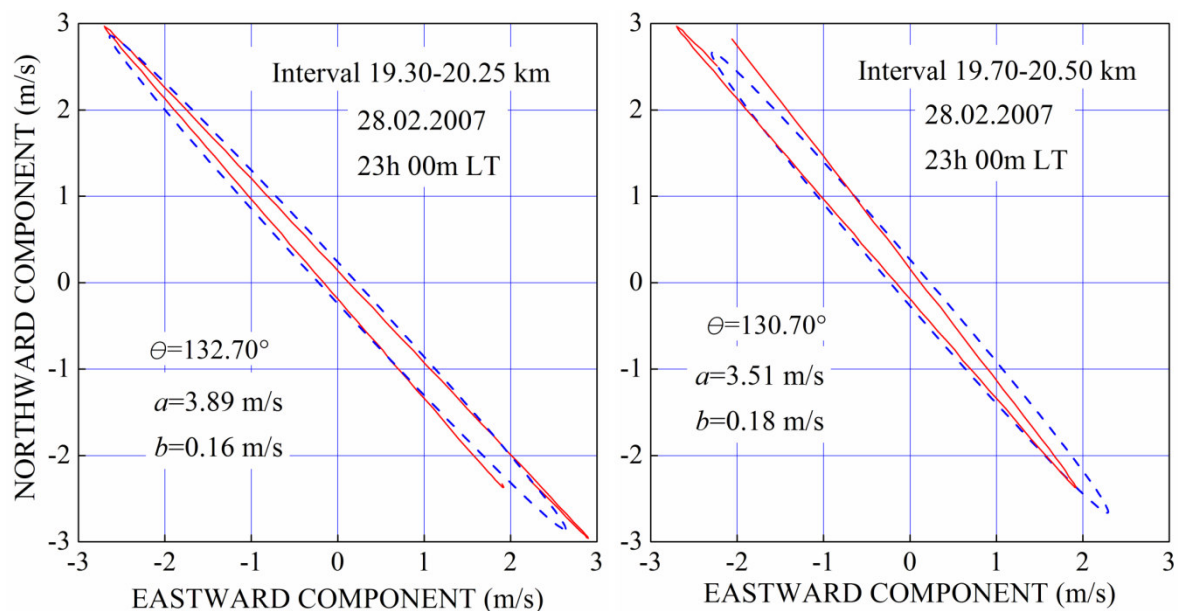

Figure 3. Results of a hodograph analysis for wind speed disturbances which were obtained from radiosonde measurements on February 28, 2007 at the Cocos Islands stratosphere in two altitude intervals 19.30–20.25 km (left panel) and 19.70–20.50 km (right panel). Lengths of major and minor semi-axes of ellipse and values of angle θ are represented in this figure.

Orientation of the hodograph ellipse major axis determines direction of the horizontal wave vector component $\mathbf{k_h}$ with an uncertainty of ±180°. It can be seen from the hodographs shown in Figures 2 and 3 that the IGW phase propagation may be in the north-west (N/W) or south-east (S/E) direction. The expression for a Doppler shift between the intrinsic frequency ω and frequency σ in the reference frame of ground-based observer has following form [25]:

$$\omega = \sigma - \mathbf{k_h}\mathbf{V_b} = \sigma - |\mathbf{k_h}|\,|\mathbf{V_b}|\cos\alpha, \tag{3}$$

where $\mathbf{V_b}$ is the background wind speed vector, $\mathbf{k_h}\mathbf{V_b}$ is the scalar product of the $\mathbf{k_h}$ and $\mathbf{V_b}$ vectors, and α is an angle between these vectors.

According to an analysis of the wind speed hodograph for five considered intervals, we obtained the mean value of azimuthal angle θ = 132.4°. We also determined the background wind speed modulus $|\mathbf{V_b}|$ = 8.6 m/s, the horizontal wave-number modulus $|\mathbf{k_h}| = k_h = 2.62 \cdot 10^{-4}$ rad/m, and the mean value of α-angle (α = 7.2°) between the vector $\mathbf{V_b}$ and the S/E-direction of hodograph major axis. These data and other internal wave characteristics are presented in Table 1. Using the expression (3) and above-mentioned values, the scalar product $\mathbf{k_h}\mathbf{V_b} = 22.36 \cdot 10^{-4}$ rad/s was found. The performed analysis shows that the north-west direction of wave phase propagation is impossible. In this case, according to (3), the modulus |ω| should be no less than the scalar product $\mathbf{k_h}\mathbf{V_b} = 22.36 \cdot 10^{-4}$ rad/s, but we determined that the mean value |ω| is equal to ω = $8.36 \cdot 10^{-4}$ rad/s (Table 1). We also calculated hypothetical frequencies σ_2 and σ_3 for two cases of wave phase propagation in the south-east (S/E) direction, when the IGW horizontal phase speed (in the reference frame of ground-based observer) is respectively less or greater than the absolute value of the mean wind speed projection onto the S/E-direction. It was assumed by us that properties of the internal wave source are weakly dependent on time, and the "true" frequency σ in the reference frame of ground-based observer should remain practically constant during the IGW propagation in the analyzed altitude range 19.0–20.5 km.
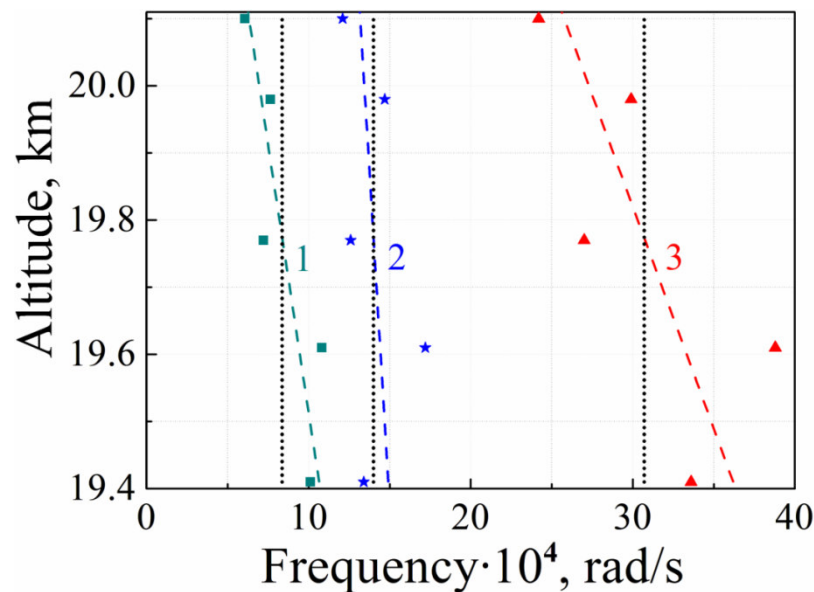

Figure 4. Magnitudes of intrinsic frequency ω (squares) and hypothetical frequencies σ_2 (asterisks) and σ_3 (triangles) calculated for two considered cases of the IGW phase propagation in the south-east direction. Mean values of frequencies are shown by dotted lines, and dashed lines demonstrate the linear altitude trends of experimental frequency data.

Figure 4 shows linear altitude trends of the intrinsic frequency ω (squares) and hypothetical frequencies σ_2 (asterisks) and σ_3 (triangles) which were calculated for two above-mentioned cases of the IGW phase propagation in south-east direction. Mean frequency values are shown by dotted lines, and the dashed lines correspond to altitude data trends obtained on the basis of a linear approximation of experimental data by the least squares method in the altitude range 19.0–20.5 km. Experimental

magnitudes of the IGW frequencies in Figure 4 refer to the middles of five altitude intervals in which the wind speed hodographs were constructed.
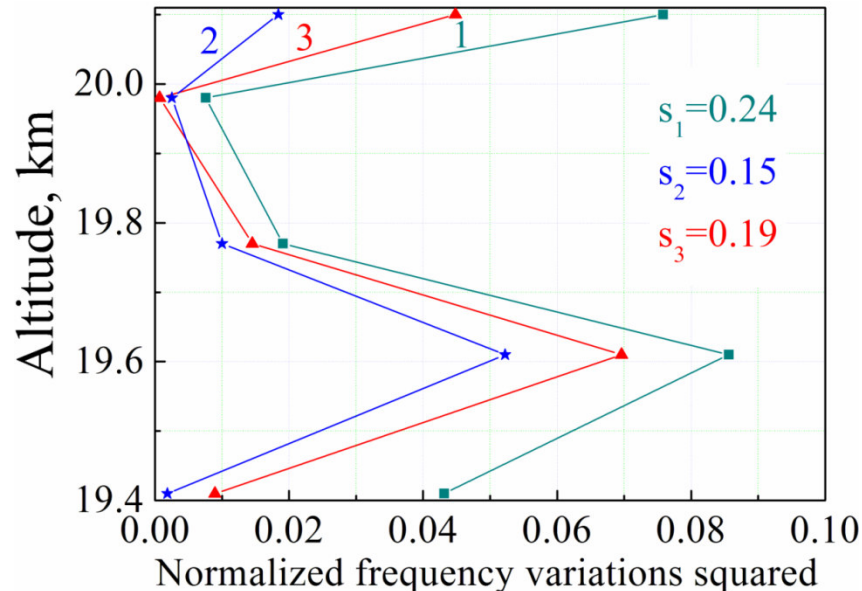

Figure 5. Vertical profiles of the normalized variations squared for the intrinsic frequency ω (squares), hypothetical frequencies σ_2 (asterisks) and σ_3 (triangles) in the reference frame of ground-based observer. Values of the normalized standard deviations (s_1, s_2 and s_3) of indicated frequencies from corresponding background values are shown in this figure.
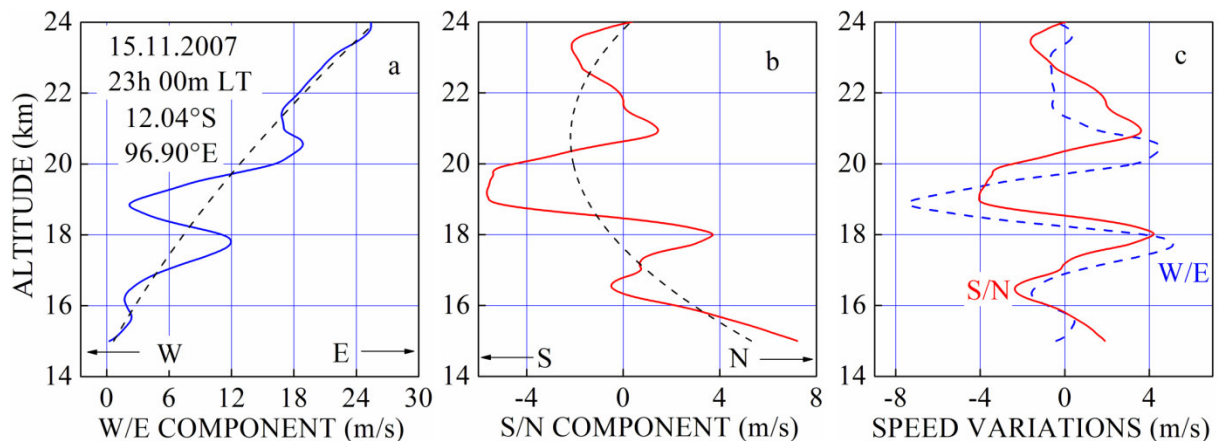

Figure 6. Altitude profiles of the zonal (W/E-component) and meridional (S/N-component) wind speed components (panels a and b) obtained from radiosonde measurements on November 15, 2007 at the Earth's lower stratosphere over Cocos Islands. Dashed lines in panels a and b denote the background profiles of wind speed components calculated using the LSM-approximation of initial data by a third-degree polynomial in the interval 15.0–24.0 km. Vertical profiles of the wind speed component variations are shown in panel c of this figure.

The altitude frequency trends shown in Figure 4 indicate that the frequency σ_2 is a conserved invariant in more extent than the frequency σ_3. This is also evidenced by the vertical profiles of normalized frequency variations and by the meanings of their standard deviations (Figure 5). Thus, setting the value $\sigma = \sigma_2 = 14.0 \cdot 10^{-4}$ rad/s as the "true" frequency in the reference frame of ground-based observer, we can conclude that in the reference system moving with the speed of undisturbed

flow, the intrinsic frequency ω is determined with a minus sign: $\omega = \sigma_2 - \mathbf{k_h V_b} = -8.36 \cdot 10^{-4}$ rad/s. This means that the analyzed internal wave propagates at north-west direction in the indicated reference system. It should be noted that in the reference frame of ground-based observer, the internal wave phase propagates in the south-east direction.
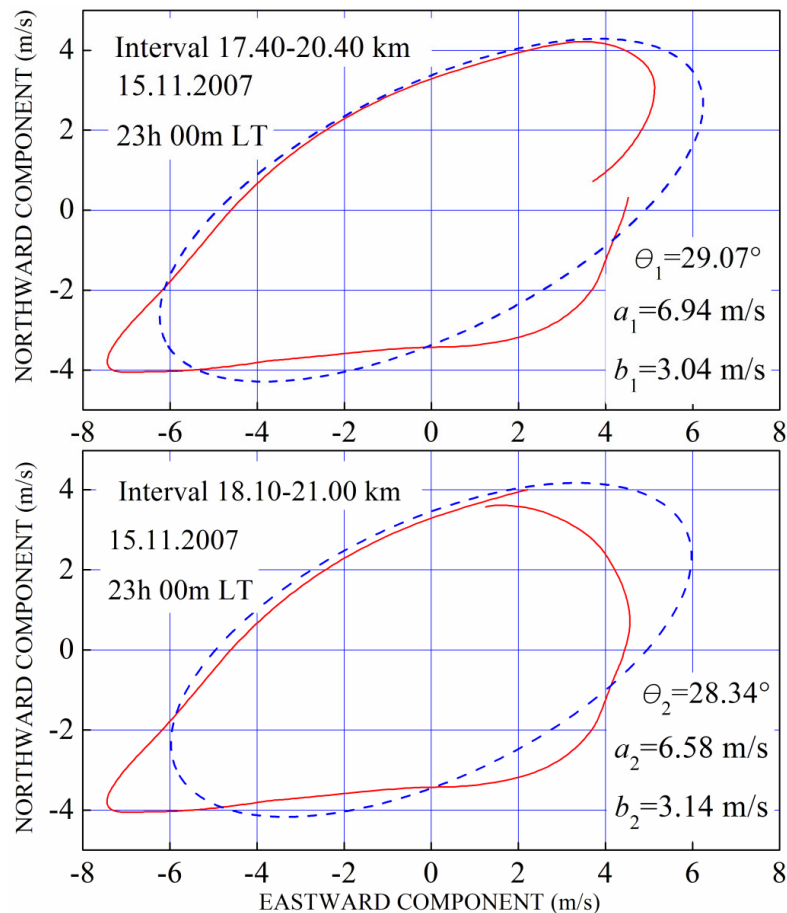

Figure 7. Results of a hodograph analysis for wind speed disturbances which were obtained from radiosonde measurements on November 15, 2007 at the Cocos Islands stratosphere in two altitude intervals 17.40–20.40 km (top of Figure 7) and 18.10–21.00 km (bottom). Description of panels is the same as in Figure 2.

Figure 6 shows altitude profiles of the zonal and meridional wind speed components (panels a and b) obtained from radiosonde measurements on November 15, 2007 at the Earth's lower stratosphere over Cocos Islands. The coordinates of sounded area and the local time (LT) of measurements are shown. The background wind speed profiles calculated using the LSM-approximation of initial data by a third-degree polynomial at the interval 15.0–24.0 km are indicated by dashed lines in panels a and b of Figure 6. Vertical profiles of variations for the wind speed components are given in panel c, and they were determined as differences between the initial and mean profiles.

Figure 7 demonstrates results of the hodograph analysis for wave disturbances of the wind speed obtained from radiosonde measurements on November 15, 2007 at the Earth's atmosphere over Cocos Islands in two altitude intervals 17.40–20.40 km (top of Figure 7) and 18.10–21.00 km (bottom). The description of panels here is the same as in Figure 2. An internal wave, identified in the radiosonde measurement session on November 15, 2007, has intrinsic period of $T^{in} = 26.3$ hours (ω =2.2·f), where $f = 3.04 \cdot 10^{-5}$ rad/s is the Coriolis parameter for observation point at the Earth's atmosphere. Vertical and horizontal wavelengths for this internal wave are ~2.95 and ~1350 km, respectively.

Table 1. Parameters of internal gravity waves reconstructed in two sessions of radiosonde measurements at the Earth's lower stratosphere over Cocos Islands using an analysis of the wind speed hodograph. Coordinates of the probed region and local times (LT) of the measurements are shown

Measurement	28.02.2007 23h 00m LT 12.04°S, 96.90°E. [19.0÷20.5] km	15.11.2007 23h 00m LT 12.04°S, 96.90°E [17.4÷21.0] km
IGW parameters		
λ_z, km	0.80	2.95
m, 10^{-3} rad/m	7.85	2.13
f/ω, rel. units	0.036	0.458
$|u'|$, m/s	3.73	6.76
$|v'|$, m/s	0.14	3.09
$|w'|$, 10^{-3} m/s	124	14.8
θ, deg	132.4	28.7
N_b, 10^{-2} rad/s	2.5	2.7
λ_h, km	24.0	1348
k_h, 10^{-4} rad/m	2.62	0.047
ω, 10^{-4} rad/s	8.36	0.664
T^{in}, hours	2.09	26.3
$\left|C_{ph}^{in}\right|$, m/s	3.19	14.25
$\left|C_{pz}^{in}\right|$, 10^{-3} m/s	106	31.2
$\left|C_{gh}^{in}\right|$, m/s	3.19	11.27
$\left|C_{gz}^{in}\right|$, 10^{-3} m/s	106	24.68
σ, 10^{-4} rad/s	14.0	–
T, hours	1.25	–
$|\mathbf{V_b}|$, m/s	8.6	–
α, deg	7.2	–
E_p, m²/s²	3.48	9.03
E, m²/s²	6.96	22.85
$p = E_k/E_p$, rel. units	1.0	1.53

Table 1 shows the internal wave characteristics obtained from an analysis of the wind speed hodograph in the measurement sessions on 28 February and on 15 November 2007. The kinetic (E_k), potential (E_p), and total (E) wave energy per unit mass are given here. Values $\left|C_{ph}^{in}\right|$ and $\left|C_{pz}^{in}\right|$ are moduli of the intrinsic horizontal and vertical phase speeds, and values $\left|C_{gh}^{in}\right|$ and $\left|C_{gz}^{in}\right|$ are moduli of the intrinsic horizontal and vertical group speeds, correspondingly. Definitions for values indicated above, and expressions for their determinations may be found in the works [27, 28].

3. Conclusion
Radiosonde wind speed measurements performed on 28 February and on 15 November 2007 were used for the identification of IGWs and determination their characteristics in the Earth's lower stratosphere over Cocos Islands (coordinates: latitude – 12.04°S and longitude – 96.90°E). Using the dispersion and polarization equations and the results of a wind speed hodograph analysis, the magnitudes of key IGW characteristics such as intrinsic frequency; amplitudes of vertical and horizontal wind speed disturbances; intrinsic vertical and horizontal phase (and group) speeds; kinetic, potential and total wave energy per unit mass were determined. Internal waves detected in these

radiosonde measurements had intrinsic periods of ~2.1 hours ($\omega = 27.8 \cdot f$) and ~26.3 hours ($\omega = 2.2 \cdot f$), respectively, where $f = 3.04 \cdot 10^{-5}$ rad/s is the Coriolis parameter for observation region at the Earth's lower stratosphere. The vertical wavelengths of identified IGWs were ~0.8 and ~2.95 km, and the horizontal wavelengths were equal to ~24 and ~1350 km, respectively. An analysis of the wind speed hodograph has shown a cyclonic (counterclockwise) rotation of a wind speed vector with increasing altitude, which corresponds to the downward phase propagation in the Southern Hemisphere and, consequently, the upward wave energy transfer. The upgraded version of hodograph method is proposed for determining the wave frequency in the reference frame of ground-based observer and the azimuthal direction of IGW propagation at the Earth's atmosphere. Application of this upgraded hodograph technique to radiosonde wind speed measurements performed on February 28, 2007 made it possible to find the actual wave frequency $\sigma = 14.0 \cdot 10^{-4}$ rad/s and period $T = 1.25$ hours, as well as other IGW characteristics in the reference frame of ground-based observer.

4. Acknowledgments

5. References

[1]   Kundu P K 1976 *J. Phys. Oceanogr.* **6** 879.
[2]   Thompson R O R Y 1978 *Q. J. R. Meteorol. Soc.* **104** 691.
[3]   Woodman R F 1980 *Radio Sci.* **15** 417.
[4]   Cot C and Barat J 1986 *J. Geophys. Res.* **91** 2749.
[5]   Gardner C S and Voelz D G 1986 *J. Geophys. Res.* **91** 3659.
[6]   Vincent R A and Fritts D C 1987 *J. Atmos. Sci.* **44** 748.
[7]   Cornish C R and Larsen M F 1989 *J. Atmos Sci.* **46** 2428.
[8]   Franke S J and Thorsen D 1993 *J. Geophys. Res.* **98** 18607.
[9]   Meriwether J W 1993 *J. Geophys. Res.* **98** 20713.
[10]   Sato K 1994 *J. Atmos. Terr. Phys.* **56** 755.
[11]   She C Y and Yu J R 1994 *Geophys. Res. Lett.* **21** 1771.
[12]   Cho J Y N 1995 *J. Geophys. Res.* **100** 18727.
[13]   Swenson G R, Gardner C S and Taylor M J 1995 *Geophys. Res. Lett.* **22** 2857.
[14]   Eckermann S D 1996 *J. Geophys. Res.* **101** 19169.
[15]   Gavrilov N M, Fukao S, Nakamura T, Tsuda T, Yamanaka M D and Yamamoto M 1996 *J. Geophys. Res.* **101** 29511.
[16]   Namboothiri S P, Tsuda T, Tsutsumi M, Nakamura T, Nagasawa C and Abo M 1996 *J. Geophys. Res.* **101** 4057.
[17]   Walterscheid R L, Hecht J H, Vincent R A, Reid I M, Woithe J and Hickey M P 1999 *J. Atmos. Sol.-Terr. Phys.* **61** 461.
[18]   Preusse P, Eckermann S D and Offermann D 2000 *Geophys. Res. Lett.* **27** 3877.
[19]   Hecht J H, Walterscheid R L, Hickey M P and Franke S J 2001 *J. Geophys. Res.* **106** 5181.
[20]   Hu X, Liu A Z, Gardner C S and Swenson G R 2002 *Geophys. Res. Lett.* **29** 2169, doi:10.1029/2002GL014975.
[21]   Ern M, Preusse P, Alexander M J and Warner C D 2004 *J. Geophys. Res.* **109** D20103.
[22]   Serafimovich A, Hoffmann P, Peters D and Lehmann V 2005 *Atmos. Chem. Phys.* **5** 295.
[23]   Rauthe M, Gerding M, Hoffner J and Lubken F-J 2006 *J. Geophys. Res.* **111** D24108.
[24]   Rauthe M, Gerding M and Lubken F-J 2008 *Atmos. Chem. Phys.* **8** 6775.
[25]   Gubenko V N and Kirillovich I A 2018 *Sol.-Terr. Phys.* **4** 41, doi: 10.12737/stp-42201807.
[26]   Gubenko V N, Kirillovich I A and Andreev V E 2021 *Journal of Physics: Conference Series* **1632** 012007, doi: 10.1088/1742-6596/1632/1/012007.
[27]   Gubenko V N, Pavelyev A G, Salimzyanov R R and Andreev V E 2012 *Cosmic Res.* **50** 21, doi: 10.1134/S0010952512010029**.**
[28]   Gubenko V N, Pavelyev A G, Salimzyanov R R and Pavelyev A A 2011 *Atmos. Meas. Tech.* **4**. 2153, doi: 10.5194/amt-4-2153-2011.